

THE UNIVERSITY OF MELBOURNE

DESIGN FOR INTEGRATION MCEN90013

DESIGN PROJECT 5

Progress Report 1

Group members:

James Osmond, 390451

Clarke Simpson, 388553

Nick Mason, 542025

Geoffrey Bullen, 390666

Joseph Rokebrand, 389894



THE UNIVERSITY OF

MELBOURNE

August 2014

Summary

- Overall layout: The final layout has been decided on. Centre distances and volume occupied are dependent on the optimization of the gears discussed below.
- Gear design: As a starting point we have found the maximum gear diameters that will allow us to remain within the volume constraints set out. We have completed all the basic calculations required to design these components of the gearbox and have some starting values which we plan on optimizing in the next phase of the design. Reduction of these gear sizes will result in a decrease in the centre distances between shafts, and most probably the cost of the gearbox. Methodology has been obtained from both Shigley's Mechanical Engineering Design and AGMA 901-A92.
- Shafts: Minimum diameter design has been undertaken, in accordance with loading specifications and safety factors as set out in AS1403-2004. This was done using bending moment and torque diagrams to find the critical points, then iteratively solving for the required diameters. Calculations for deflection of shafts are underway however some work still remains to be done in this section.
- Bearings: Calculations of minimum required life rating have been made and appropriate bearings selected. These calculations included the radial loads as axial stress is minimal due to double helical configuration
- Heat: A qualitative examination of heat production has been performed to identify major producers and dissipaters of heat.
- Vibration: The method for the vibration analysis has been detailed in this document, taking into consideration the natural frequencies in both torsion and lateral directions. Full analysis has not yet been completed.
- Assembly: The method of assembly although not detailed, is to have a two piece gearbox housing to allow easy shaft, gear and bearing insertion.

Contents

1	Gear Design Overview	3
1.1	Spur	3
1.2	Helical	3
1.3	Decision	3
1.4	Hunting tooth convention	4
2	Gear Geometry Analysis	4
2.1	Compound two stage train design	4
2.2	Gear Ratio Selection for Minimum Volume Design	4
2.3	Compound spur two stage with idler gear train design	5
2.4	Gear Train Force and Stress Analysis	5
3	Shaft Design	7
3.1	Force Analysis	7
3.2	Shaft Material Selection	8
3.3	Shaft Diameter Calculations	9
3.4	Discussion of Reults	17
3.5	Shaft Deflection Analysis	17
4	Bearing Selection	17
5	Retaining Ring and Keyway Selection	18
6	Design Layout	18
6.1	Selection of Gearbox Layout	18
6.2	Preliminary Drawings	18
6.3	Manufacture of a Scale Prototype	18
7	Vibrational Analysis	21
7.1	Prospective Analysis	21
8	Thermal Analysis	22
9	Progress Review	24
	Appendices	24
A	Minimum Volume Gear Design	28
B	Shafts	29
B.1	Australian Standard Shaft Equations	29
B.2	Shaft Forces	30
B.3	Shaft Free Body Diagrams	31
B.4	Shaft Bending Moment and Torque Diagrams	33
C	SIN Diagrams	37
D	Gantt Charts	40
E	References	42

1 Gear Design Overview

1.1 Spur

Spur gears are simplest type of gear. The teeth of a spur gear are projected radially and are parallel to the axis of the gear. Each tooth is exactly perpendicular to the face of the gear it protrudes from. These gears will only mesh together correctly if their shafts are parallel.

Pros	Cons
Simpler to manufacture – As spur gears are significantly simpler to manufacture they are in turn less expensive as less time is spend in the design process.	They are nosier at high speeds – it is a tradeoff between efficiency and noise in this case.
The 0 degrees between the contact points of spur gears means they are very efficient as the entire surface area engages at once.	They are not flexible in terms of room constraints – The shafts must be parallel.
They are very robust – Due to their simple nature and construction Spur gears are notoriously reliable.	In certain cases special types of lubricant are necessary for the long term successful application of helical gears.

1.2 Helical

The teeth of helical gears are not parallel to the gear axis; they are set at an angle. Since the surface over which the teeth are made is cylindrical, the teeth form the shape of a Helix. It is important to make the distinction between the two major subsets of helical gears. There exists, ‘Cross-Axis’ helical gears, where the axes of the shafts are non-intersecting and greater than 0° apart (usually 90°) and then, there are ‘parallel-axes’ helical gears. These are more self-explanatory in that the axes upon which the gears sit are parallel to each other. For the purposes of the current discussion we will be examining the latter of the two and the pros and cons associated with the use of them in a polyethylene mixer gearbox.

Pros	Cons
Helical gears are significantly quieter – The teeth engage in a gradual manner than the entire face at once.	Difficult to manufacture due to the angled teeth on the gear, depending on the manufacturing process this can become a major factor.
They are able to withstand a higher load for equivalent width and tooth size. – The effective length of the tooth is increased due to its diagonal nature.	Generation of thrust load due to angled contact from one gear
If required, they can be made to engage at difference angles – this can provide flexibility in layout and help designers comply with size restraints. NOTE: Efficiency decreases as the angle between the gear axes increases.	In certain cases special types of lubricant are necessary for the long term successful application of helical gears.

1.3 Decision

By acknowledging that both Helical and Spur have advantages and disadvantages the prospect of utilizing both gears on one gearbox could prove to be the best option. The input shaft of the poly mixer has a relatively high rotation in comparison to the output shaft so we propose that on the input shaft a double helical gear is used. Once the slower rotational speed has been reached it then seems fit to utilize the cheaper manufacturing benefits and robust nature of a spur gear.

1.4 Hunting tooth convention

The Hunting Tooth convention states that no two teeth on meshing gears should make contact with each other more regularly than with any other tooth. Mathematically this means that the number of teeth on each gear in a mesh should have no common factors with each other. This ensures that all teeth make contact with each other evenly and no abnormal wear will occur. The Hunting Tooth convention is employed to minimise the risk of two damaged teeth repeatedly coming into contact with each other. Therefore all ratios considered in the coming Analysis have no factors in common and are referred to as Hunting Tooth Ratios or as satisfying the Hunting Tooth Convention.

2 Gear Geometry Analysis

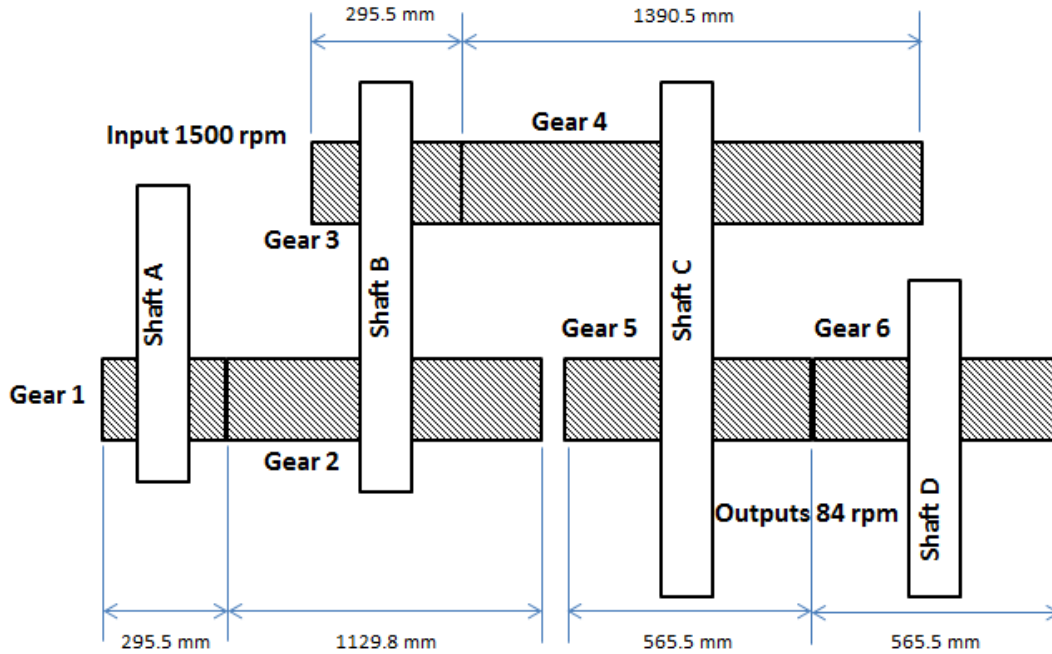


Figure 1: Initial Gearbox Layout

2.1 Compound two stage train design

After completing a series of preliminary size calculations, it was confirmed that a conventional two-stage system would be adequate. This is largely due to the fact that the input-output shaft distance, maximum gear size and gear ratio constraints could all be simultaneously satisfied. The initial layout is shown in figure 1. Note that shaft A will sit directly on top of shaft B in our final design, satisfying the size constraint of the gearbox.

2.2 Gear Ratio Selection for Minimum Volume Design

Having more than one reduction in a gearbox, a major decision is how to split the gear ratios. By minimizing the volume of the gears, it reduces the weight and likely the cost of the gearbox. As per AGMA 901-A92 (A Rational Procedure for the Preliminary Design of Minimum Volume Gears) the resulting gear ratios were 3.79 and 4.71 (for double helical gears). These values have been used for further gear calculations discussed later. For the methodology and assumptions used in finding these ratios please see the calculation section in the appendices.

2.3 Compound spur two stage with idler gear train design

Consideration 1: Selection of a standard gear module

A secondary factor considered when determining the choice of module in this design, was the possibility of using different m values for each stage in the system. The driving force experienced by the teeth in mesh is constant for all gears within a stage. Since the first stage is driven at the input, its forces will be a direct function of the torque produced by the motor. Contrarily, the forces experienced by the gear teeth throughout the second stage will be a function of torque on the compound axle; which is being driven by the largest gear from the first stage (i.e. this is the nature of compound gearing systems). Since there will be an inherent difference in the size of radii between the two gears connected to the compound shaft (i.e. the largest gear from stage 1 and the smallest gear from stage 2), the forces in stage two are expected to be considerably larger when considering that the torque is constant along the shaft. Thus, it is reasonable to design the second stage with a higher module value than the first stage.

Consideration 2: Determining the ratio split between stages

As suggested above, it is apparent that the forces experienced by the teeth in the second stage will be larger than those of the first stage; as a result of the constant torque on the compound shaft. For this reason, it is desirable to have a comparatively small difference in the gear radius size between the two gears connected to this axle (i.e. the largest gear from stage 1 and the smallest gear from stage 2). By minimising this radius ratio, the forces experienced in stage two will inherently be minimised. This is mathematically represented as follows:

$$T_{CompoundShaft} = r_{Gear,1}W_{t1} = r_{pinion,1}W_{t2}$$

$$W_{t2} = \frac{r_{gear,1}}{r_{pinion,1}}$$

Since the radius of the larger gear in stage 1 is a function of the stage ratio, it is desirable to split the overall gear train value, such that the first stage increases by a smaller amount than the second. This will effectively reduce the radius ratio between the two gears connected to the compound shaft (and therefore minimise the forces acting on the teeth in stage 2). However, it is important to note that by decreasing the ratio split at stage one, the ratio for stage two will consequently increase; meaning that a larger gear diameter will be required to achieve an overall value of approximately 17.857:1. Thus, it is important to ensure that the maximum allowable gear diameter constraint is still satisfied.

Consideration 3: Selecting the number of pinion teeth for each stage

The next free variable to consider in the gearbox design is the number of teeth for each pinion in the train. As previously discussed, the number of pinion teeth is directly related to both the module and pinion diameter.

$$Diameter = m(numberofteeth)$$

For a selected module value, adjusting the number of teeth will vary the overall diameter of the pinion. This is significant when considering the forces that propagate through the system. The driving force experienced by the gears in stage one can be calculated according to the torque produced by the motor.

2.4 Gear Train Force and Stress Analysis

Having determined the respective reduction ratios, numbers of teeth and general layout of the gearbox, an analysis of the forces and stresses acting on individual gears can be carried out. This analysis is performed in accordance with the AGMA guidelines for gear stress calculations, specifically the AGMA stress equations for bending and pitting resistance, shown in Equations 1 and 2 respectively.

$$\sigma = W^t K_o K_v K_s \frac{P_d}{F} \frac{K_m K_B}{J} \quad (1)$$

$$\sigma_c = C_p \sqrt{W^t K_o K_v K_s \frac{K_m C_f}{d_p F} \frac{1}{I}} \quad (2)$$

It can be observed that these equations take into account a number of factors, which themselves depend on a number other variables, and hence we sought to develop a system of obtaining valuable results from these equations whilst also tracking inputs in order to make future iterations simple. This was achieved through the creation of an electronic spreadsheet to list all input variables and corresponding results, as well as all assumptions made in the analysis process. This process obtained results including transmitted force between each gear couple and contact and bending stress on each of the six individual gears. The main results are summarized below in Table 1, and a printout of the spreadsheet used to calculate them is attached in the appendices.

	Transmitted Force (kN)	Transmitted Torque (kNm)	Contact Stress (psi)	Contact Stress (MPa)	Bending Stress (psi)	Bending Stress (MPa)
Gear 1	108.95	10.06	194995	1344.44	54378	374.93
Gear 2	108.95	38.46	194995	1344.44	38462	265.19
Gear 3	416.56	38.46	359503	2478.69	173326	1195.04
Gear 4	416.56	181.01	359503	2478.69	119677	825.15
Gear 5	640.18	181.01	364495	2513.11	145997	1006.62
Gear 6	640.18	181.01	364495	2513.11	145997	1006.62

Table 1: Summary of force and stress analysis results

It should be noted that these results represent our approximation for input variable values, including those for diametral pitch, respective gear diameters, and the numerous factors included in the AGMA equations. We expect to further increase the reliability of these results as we explore alternate combinations of variables, and gain a greater understanding of the underlying factors outlined in the AGMA standards. These iterative calculations will be aided greatly by our automated spreadsheet. Moving forward, the results gained from this analysis are integral to the development of shaft design for the gearbox, as well as the choice of material and hardening technique for individual components, which will be the subject of further analysis in the near future.

3 Shaft Design

Figure 2 shows the initial layout of the shafts. The objective of the shaft design is to specify the diameter along each shaft which will allow the shaft to resist the forces applied on it by the gears with a factor of safety of 2.5. The shaft design process is stepped out below.

1. Identify the forces acting on each shaft and construct free body diagrams
2. Calculate the bending moments and torques acting on each shaft (done by creating bending moment and torque diagrams)
3. Select the shaft material and identify material properties
4. Select the required safety factor
5. Calculate the required diameter at critical sections along each shaft.

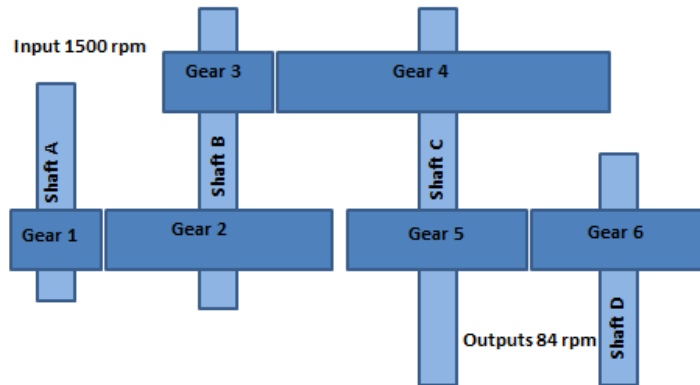


Figure 2: Initial shaft layout

In our initial calculations, it was assumed that all bearings were located in the same z axis position meaning there was no middle wall supporting the shafts. It was also assumed that all gears and shafts were on the same plane. For our final design we anticipate that shaft A will be located directly above shaft B to satisfy the gearbox size constraint. We may also place a middle wall in order to provide shaft support and further minimise gearbox volume however further study is required to determine if this is a worthwhile design. In any case the design used for our initial calculations represents the most conservative design and one upon which we can implement optimizations in the next phase of our design.

3.1 Force Analysis

The forces applied to each shaft by the meshing gears is calculated in the gear section of this document and summarised below in table 12. All forces were assumed to be point forces acting at the centre of the associated gear or bearing. Also, the weight forces of the gears and shafts are neglected as they are insignificant compared to the forces applied by the meshing gears. Also the moment of inertia of each component was ignored to keep our first run solution simple.

Appendix B.2 shows the forces acting on each shaft. From this, free body diagrams were drawn for each shaft as shown in Appendix B.3. Appendix B.4 shows the bending moment and torque diagrams of each shaft which were calculated from the free body diagrams. These are used later on to calculate the required diameters along each shaft section.

Table 2: Reaction Forces (kN)

Shaft A	Bearing a	Rax	-19.23	Shaft C	Bearing e	Rex	-193.95
		Ray	-48.85			Rey	385.80
		Raz	0			Rez	0
	Bearing b	Rbx	7.00		Bearing f	Rfx	-133.81
		Rby	17.78			Rfy	-5.96
		Rbz	0			Rfz	0
Shaft B	Bearing c	Rcx	8.99	Shaft D	Bearing g	Rgx	-167.18
		Rcy	122.39			Rgy	459.34
		Rcz	0			Rgz	0
	Bearing d	Rdx	60.99		Bearing h	Rhx	-65.82
		Rdy	206.03			Rhy	180.84
		Rdz	0			Rhz	0

Table 2 summarises the reaction forces on the shafts caused by the bearings. These forces were again modelled as point loads and this information is used later on to select appropriate bearings.

3.2 Shaft Material Selection

Table 3 shows a preliminary summary of the candidate shaft materials and their properties.

Table 3: Possible Shaft Materials

Material	Ultimate Tensile Strength (MPa)	Endurance Strength (MPa)
Low Strength Steel 1020	500	225
Medium Strength Steel 1045	780	350
Stainless Steel 410	760	342
High Tensile Steel 4340	1000	450

For our initial calculations, we selected AS1020, a cheap, readily available material which is commonly used in shaft design. This is also the safest choice for our initial calculations, as using a stronger material will result in decreasing diameters which is good for our volume constrained design. Further research will investigate the trade-off between the cost of a more expensive material versus the saving in material gained by requiring a smaller diameter.

3.3 Shaft Diameter Calculations

Process

The calculation of shaft diameter followed the process laid out in Australian Standard 1403-2004 Design of Rotatin Steel Shafts which is shown in figure 3.

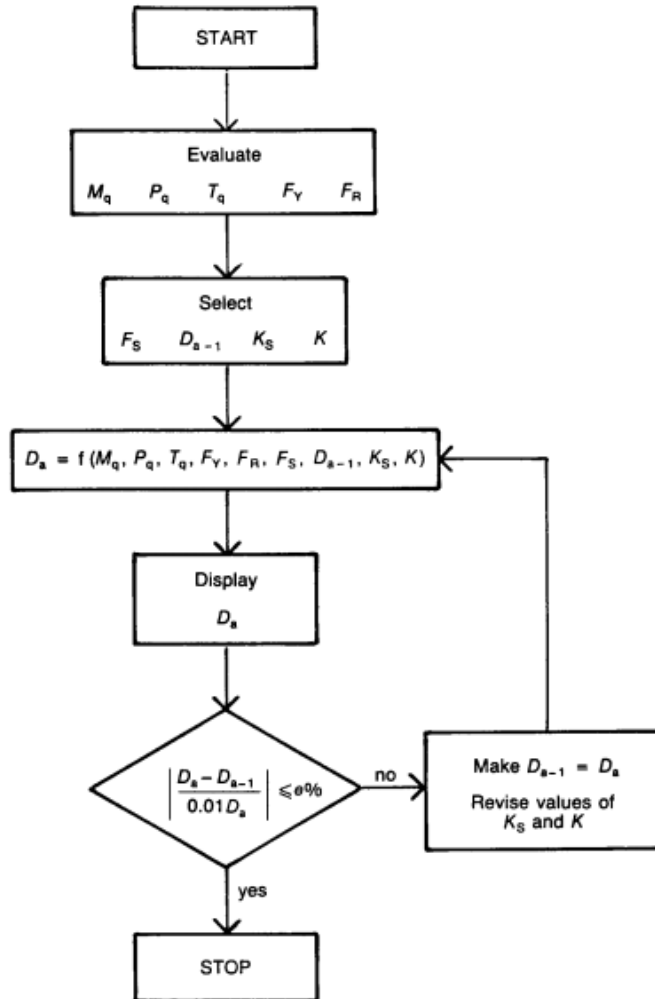


Figure 3: Shaft Diameter Iteration Process

- M_q, P_q and T_q represent the bending moment, axial load and torque on the relevant point of the shaft
- F_y and F_r represent the yield strength and endurance limit of the selected material
- F_s represents the safety factor, in this case $F_s=2.5$
- D_{s-1} represents the trial diameter used in to iteratively solve for the shaft diameter D_s
- K_s is the size factor and K is the stress raising factor associated with the geometry of the shaft
- the value of e represents how accurate our trial diameter was. For our first run calculations a value less than 2 was deemed acceptable. Further iteration would lead to a smaller e value however the accuracy gained is not required at this stage.

Equation 3 was used to calculate the required diameters along each shaft and was taken from table 2 of the Australian Standard for the Design of Rotating Steel Shafts (AS 1403 - 2004) which is shown in appendix B.1. This equation was chosen as the appropriate equation for the specified gearbox. The load cycle runs every 100 seconds and the gearbox is designed to operate non-stop over a 20 year period, it is therefore expected that there will be more than 600 mechanism starts per year. We also expect the shafts to undergo more than 900 revolutions per year and know that the gearbox is only designed to operate in one direction meaning there are no torque reversals applied to the system.

$$D^3 = \frac{10^4 F_S}{F_R} \sqrt{\left[K_S K \left(M_q + \frac{P_q D}{8000} \right) \right]^2 + \frac{3}{16} \left[(1 + K_S K) T_q \right]^2} \quad (3)$$

The initial trial diameter D_{s-1} was selected using figure 4 taken from AS 1403-2004. If this trial diameter did not lead to a sufficiently small e value, then the calculated diameter was taken to be the trial diameter and calculation process reiterated. The material chosen for our first run calculations qualifies as low strength steel so the upper curve was used.

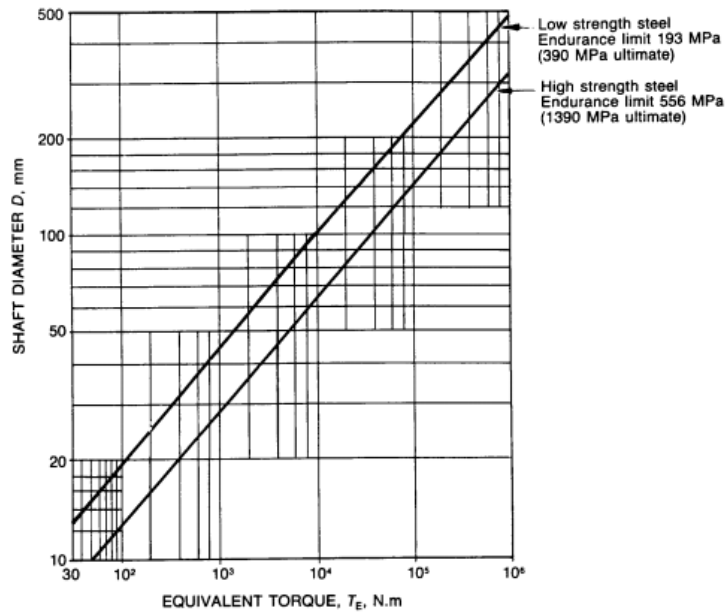


Figure 4: Trial Diameter Selection Chart

The size factor K_s was selected based on the trial diameter. We used figure 5 from AS 1403 - 2004 to select the appropriate values. The stress raising factor K is dependent on the geometry of the shaft and is influenced by factors such as stepped diameters, grooves and keyways. For our first run calculations we did not include keyways in our shaft design, and no diameters were known making it impossible to determine the effect of stepped diameters on the shaft. As a result, a conservative value of 1.5 was chosen for all calculations. When these calculations are redone for the final report, the appropriate stress raising factors will be used.

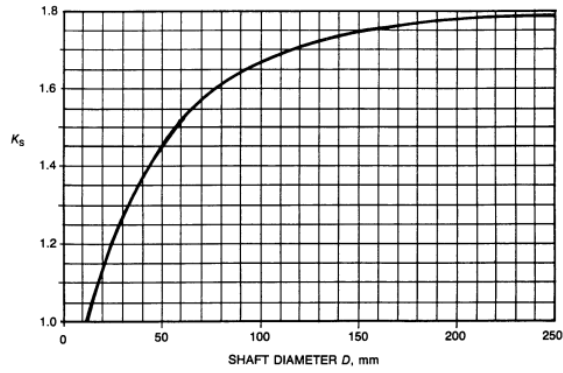


Figure 5: Size Factor (K_s) Selection Chart

Taking into account only the stepped diameter stress raising effect, figure 6 is used to select a correction factor, which can then be used in conjunction with figure 7 to a stress raising factor K .

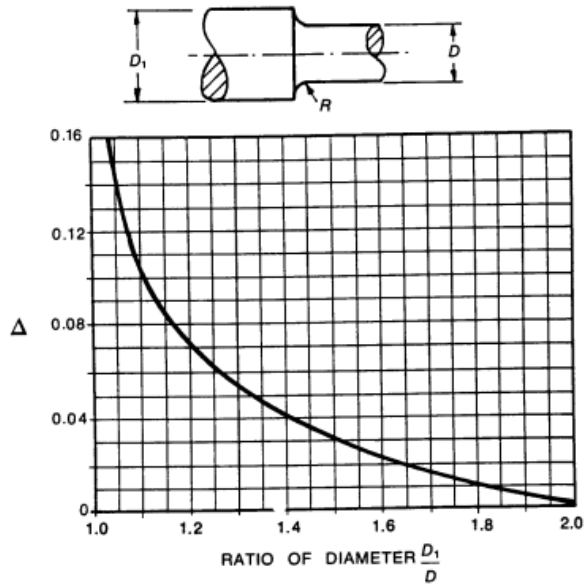


Figure 6: Correction Factor Selection Chart

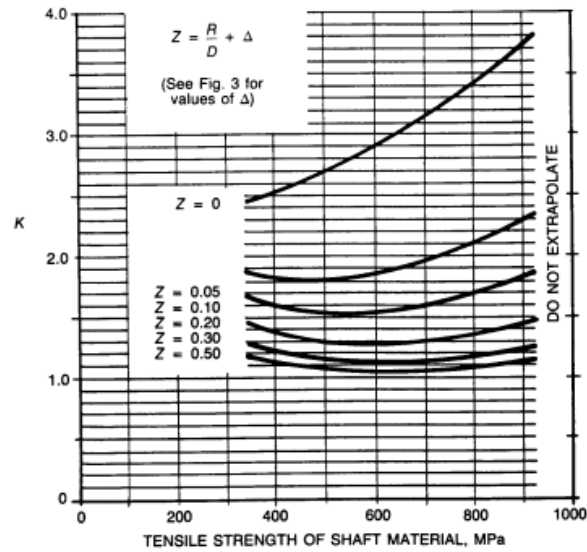


Figure 7: Stress Raising Factor Selection Chart

This process of iteratively solving for the diameter of the shaft was applied to critical sections along the shaft to reduce the diameter where possible while still meeting the safety factor requirement. In practice this was accomplished by writing a Matlab function to semi-automate the process. Critical points are chosen as the points which have high loads and or stress raising geometry present, such as on shoulders.

On all shafts shoulders were used in the design to help fix gears and bearings in place. The widest sections of each shaft were designed especially for this purpose. A ratio of $D/d=1.2$ was used to design these shoulders, where D represents the big diameter, and d the smaller diameter. This provides enough material to resist any axial forces that may arise.

Shaft A

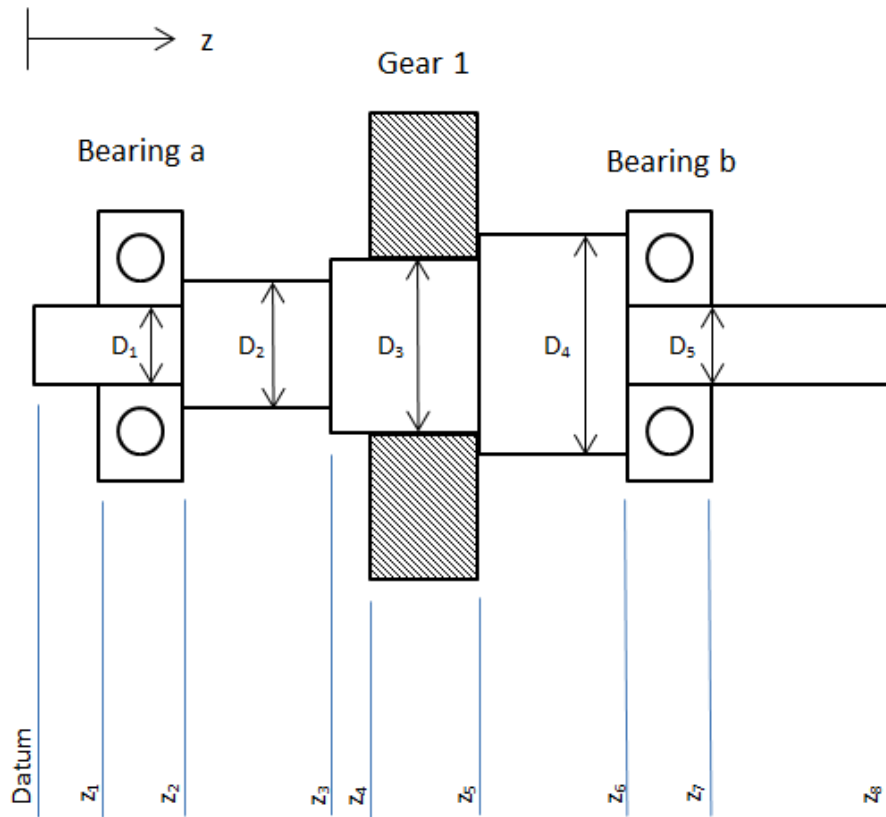


Figure 8: Shaft A

Table 4: Shaft A Diameter Calculations (mm)

Point	Dist.	M (kN)	T (kN-m)	P (kN)	Critical D	D trial	Ks	K	D final	e
z1	50	0	0	0	not critical					
z2	90	1.04	0	0	D1	63	1.53	1.5	64.25	1.94
z3	110	2.08	0	0	D2	82	1.58	1.5	81.82	0.22
z4	140	3.64	0	0	not critical					
z5	391.33	7.63	10.06	0	D3	138	1.72	1.5	140.79	1.98
z6	742.66	0.46	10.06	0	D5	118	1.7	1.5	119.89	1.58
z7	782.66	0	10.06	0	not critical					
z8	832.66	0	10.06	0	not critical					

Table 5: Shaft A Selected Diameters (mm)

Section	Selected Diameter (mm)	Section	Selected Diameter (mm)
D1	65	D4	168
D2	82	D5	120
D3	140		

Shaft B

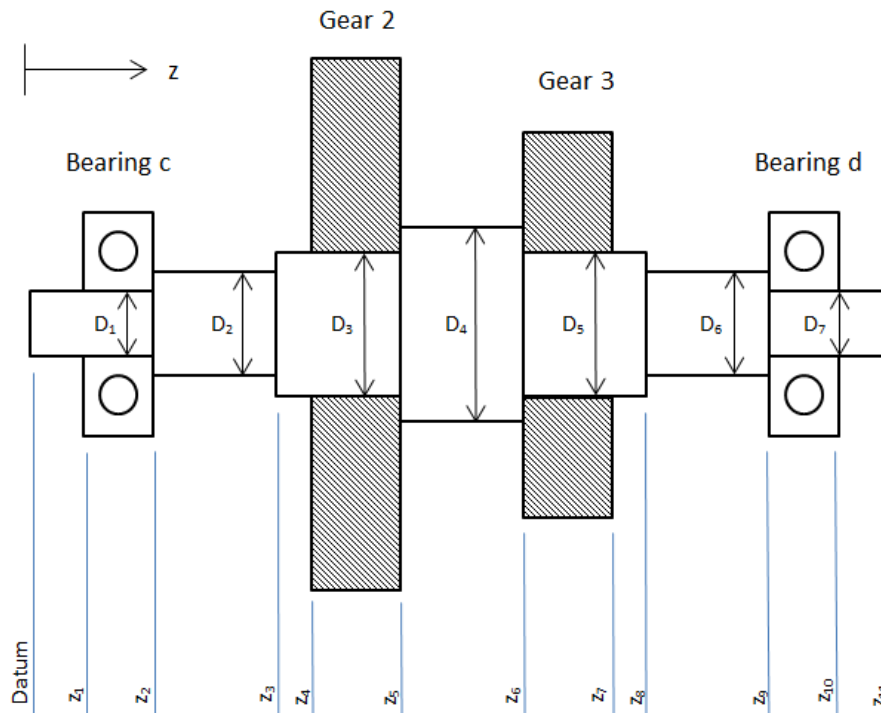


Figure 9: Shaft B

Table 6: Shaft B Diameter Calculations (mm)

Point	Dist.	M (kN)	T (kN-m)	P (kN)	Critical D	D trial	Ks	K	D final	e
z1	50	0	0	0	not critical					
z2	90	2.45	0	0	D1	86	1.6	1.5	86.7	0.89
z3	110	4.91	0	0	D2	110	1.7	1.5	111.6	1.46
z4	140	8.59	0	0	not critical					
z5	391.33	31.27	-76.93	0	D3	250	1.78	1.5	254.3	1.70
z6	441.33	34.28	-76.93	0	D5	255	1.8	1.5	257.8	1.07
z7	692.66	15.61	0	0	not critical					
z8	722.66	9.16	0	0	D6	138	1.72	1.5	138.0	.03
z9	742.66	4.87	0	0	D7	110	1.7	1.5	111.3	1.19
z10	782.66	3.61	0	0	not critical					
z11	832.66	3.48	0	0	not critical					

Table 7: Shaft B Selected Diameters (mm)

Section	Selected Diameter (mm)	Section	Selected Diameter (mm)
D1	87	D5	258
D2	112	D6	138
D3	255	D7	112
D4	310		

Shaft C

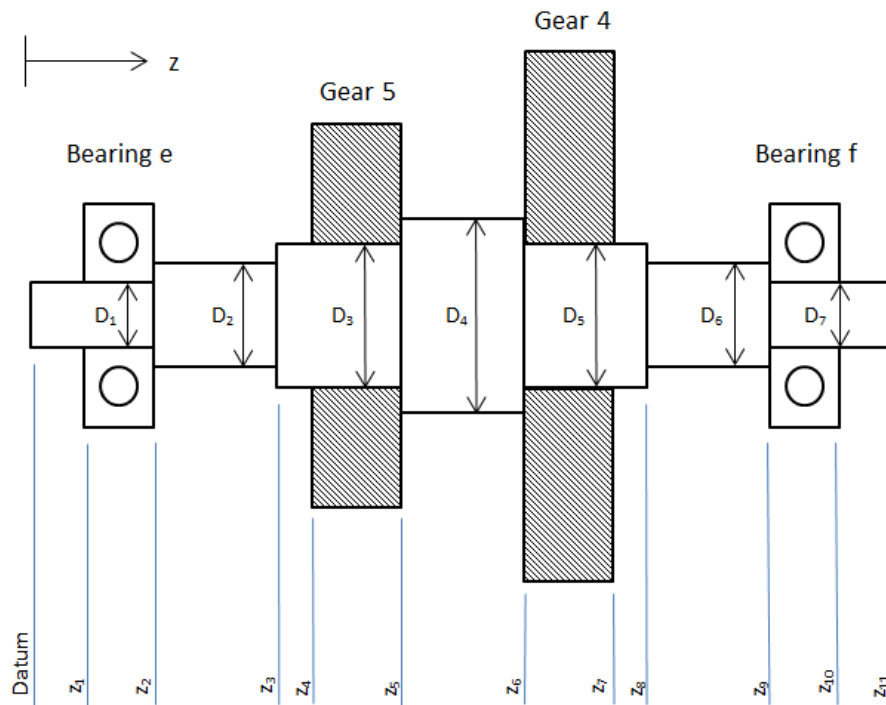


Figure 10: Shaft C

Table 8: Shaft C Diameter Calculations (mm)

Point	Dist.	M (kN)	T (kN-m)	P (kN)	Critical D	D trial	Ks	K	D final	e
z1	50	0	0	0	not critical					
z2	90	8.64	0	0	D1	135	1.72	1.5	135.56	0.41
z3	110	17.27	0	0	D2	170	1.76	1.5	171.75	1.02
z4	140	30.23	0	0	not critical					
z5	391.33	54.94	-371.47	0	D3	400	1.80	1.5	408.45	1.97
z6	441.33	44.04	-371.47	0	D5	400	1.8	1.5	407.01	1.72
z7	692.66	9.73	0	0	not critical					
z8	722.66	5.71	0	0	D6	116	1.68	1.5	116.93	0.80
z9	742.66	3.04	0	0	D7	93	1.65	1.5	94.20	1.28
z10	782.66	0	0	0	not critical					
z11	832.66	0	0	0	not critical					

Table 9: Shaft C Selected Diameters (mm)

Section	Selected Diameter (mm)	Section	Selected Diameter (mm)
D1	136	D5	410
D2	172	D6	118
D3	410	D7	95
D4	492		

Shaft D

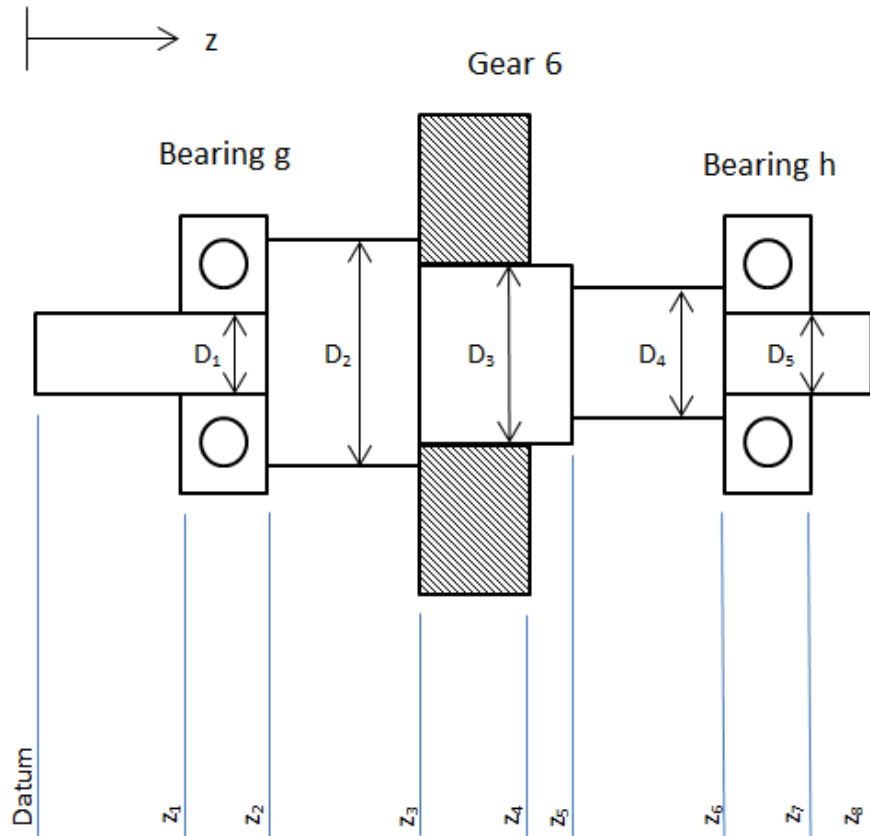


Figure 11: Shaft D

Table 10: Shaft D Diameter Calculations (mm)

Point	Dist.	M (kN)	T (kN-m)	P (kN)	Critical D	D trial	Ks	K	D final	e
z1	50	0	181.00	0	not critical					
z2	90	9.78	181.00	0	D1	318	1.80	1.5	318.65	0.83
z3	140	34.22	181.00	0	D3	320	1.80	1.5	323.38	1.04
z4	391.33	71.72	0	0	not critical					
z5	421.33	65.94	0	0	D4	270	1.80	1.5	270.45	0.16
z6	742.66	4.36	0	0	D5	105	1.68	1.5	106.88	1.76
z7	782.66	0	0	0	not critical					
z8	832.66	0	0	0	not critical					

Table 11: Shaft D Selected Diameters (mm)

Section	Selected Diameter (mm)	Section	Selected Diameter (mm)
D1	320	D4	270
D2	390	D5	108
D3	324		

3.4 Discussion of Results

The initial shaft diameters range from 65 mm to 410 mm, with larger diameters being required in the later shafts due to the higher torque forces as well as larger diameters being required in the middle of shafts due to high bending moments.

These initial diameters seem to be on the large side, however none are larger than the calculated gear diameters so this remains a viable design. If it is found that smaller diameters are preferable then a stronger material will be chosen.

3.5 Shaft Deflection Analysis

Shaft deflection analysis has not been completed at this stage. In the next design phase the deflection of the shafts under worst case loading will be analysed to check that they are within a safe tolerance. This Analysis will then be used to conduct a vibrational analysis and to ensure natural vibrational frequencies are avoided.

4 Bearing Selection

Bearings have been placed at each end of the shafts as shown in figures such as ???. The location and width of these bearings has been approximated to be used in the calculations for shaft diameters and shaft loads. Key in the decision of selecting appropriate bearings is the types of forces they will be exerted to. Also a factor is the use of double helical gears. As these gears are self aligning, over constriction of gear meshes can cause problems with teeth alignment. Hence it is advisable to allow some axial movement between the gears in each mesh. Equation 4 is used to determine the required dynamic loading rating on the bearing.

$$C_{10} = F_{eq} \left(\frac{L_d}{L_r} \right)^{\frac{1}{a}} \quad (4)$$

where:

L_d is the required life (revolutions)

L_r is the catalogue life (revolutions) equal to 10^6 for SKF

a is equal to 3 or 10/3 for ball and roller bearings respectively

This calculated value of C must then be compared with the range of available bearings, and a bearing with a higher C_{1p} is selected. The catalogue that these bearings came from is the SKF Spherical roller bearings available at

Bearing label	Shaft Diameter (mm)	Required C ₁₀ (N)	Bearing Type	Bearing Serial
a	65	953853	Cylindrical	22213CC
b	120	347180	Cylindrical	24024 CC
c	87 (95 mm)	1.4950 *10 ⁶	Cylindrical	22319CC
d	112 (120 mm)	2.6177 *10 ⁶	Cylindrical	22325CC
e	136 (140 mm)	3.3047*10 ⁶	Cylindrical	22328CC
f	95	1.025110 ⁶	Cylindrical	22319CC
g	320	3.7409*10 ⁶	Cylindrical	24168CAC
h	108 (110 mm)	1.4728*10 ⁶	Cylindrical	22322CC

Figure 12: Table of ratings and bearings used for early iteration

5 Retaining Ring and Keyway Selection

6 Design Layout

6.1 Selection of Gearbox Layout

One of the initial cornerstones of designing the gearbox, the layout was carefully selected to meet a number of criteria. Given that it was chosen well before any other detailed calculations had been attempted, several deciding factors were determined to help compare the different proposals. These included;

- 2 stage reduction for simplicity and reliability
- Minimising the torque loads on components where possible
- Even wear of all components, so that no two gears of the same dimension are under different loads
- Expandability; so that the gearbox can easily be scale up/down to accommodate increases in shaft sizes and loads
- Possibility of using a wet sump lubrication system to reduce components/wear
- Manufacturability; the ease with which it is to implement the layout in reality
- Minimised forces on the housing

The layout shown in Figure ?? was selected as the most appropriate because it best met our selection criteria. Without knowing the required shaft diameters, this layout allows us to scale up the design considerably if need be to make the second stage pinion gear large enough to satisfy the minimum space design. Due to its construction, scaling certain areas is also less likely to cause clashes with other gears/shafts in the gearbox.

The option to move away from the horizontally aligned shafts also allows for extra space to be utilised, and for the bottom of the bull gears to be submerged in the same amount of oil should wet sump lubrication be used. By selecting a layout that incorporates double helical gears on the reductions gives the option of utilising the benefits of helical gears, but without the associated axial forces placed on components such as shafts, bearings and the housing. In the end this allows for the use of a modern and technical gearseat with few of the drawbacks it would otherwise lead to. Should this be deemed too complicated or time becomes an issue it also means that the gears can be swapped for straight cut spur gears if necessary.

6.2 Preliminary Drawings

Preliminary drawings of the gearbox have been produced and can be seen below. Though they are not yet very advanced, some significant manipulation has been done in order to calculate all of the required dimensions in Matlab and have this information automatically update the 3 dimensional model in Solidworks. The benefit of this ease of updating is the ease of visibly checking for clashes and discrepancies in the results from our simulation code. This is especially useful given the number of iterations required to ensure that the whole gearbox fits together nicely and in a way that is possible to manufacture. It also means that not much more time must be spent updating CAD models/sketches for the rest of the design process, and that even those team members less familiar with the CAD process can see their changes in real time. Below are some examples of the early CAD progress:

6.3 Manufacture of a Scale Prototype

In order to successfully complete this project, a working scale prototype must also be produced. A suitable ratio of 10:1 has been chosen as a likely scale for the finished product. This size should be manageable (i.e. approximately 250mm long, 180mm high, 200mm deep), very easy to scale, yet be large enough to show all of the key details of the gearbox design. Due to the materials available, budgetary requirements and the limited access to machines, the prototype model cannot be made using the same methods as the final product. For this reason, a new method must be found for each component of the scale model;

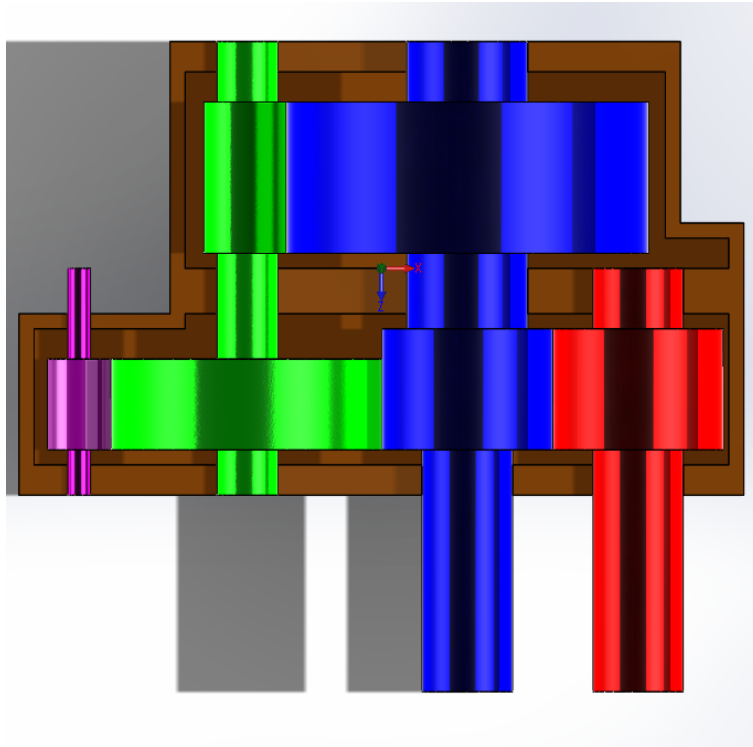


Figure 13: Top view of the selected geartrain layout with the cutaway housing

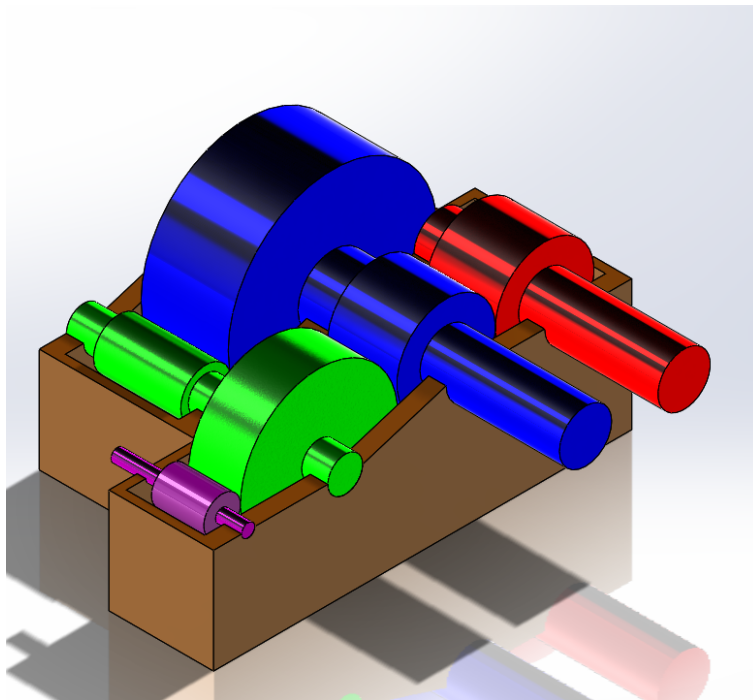


Figure 14: Isometric view of the selected geartrain layout

Housing

Due to tolerancing and reliability issues associated with 3D printing such larger components with the printers available to us, the housing is expected to be laser cut from acrylic and glued together. Whilst it means that

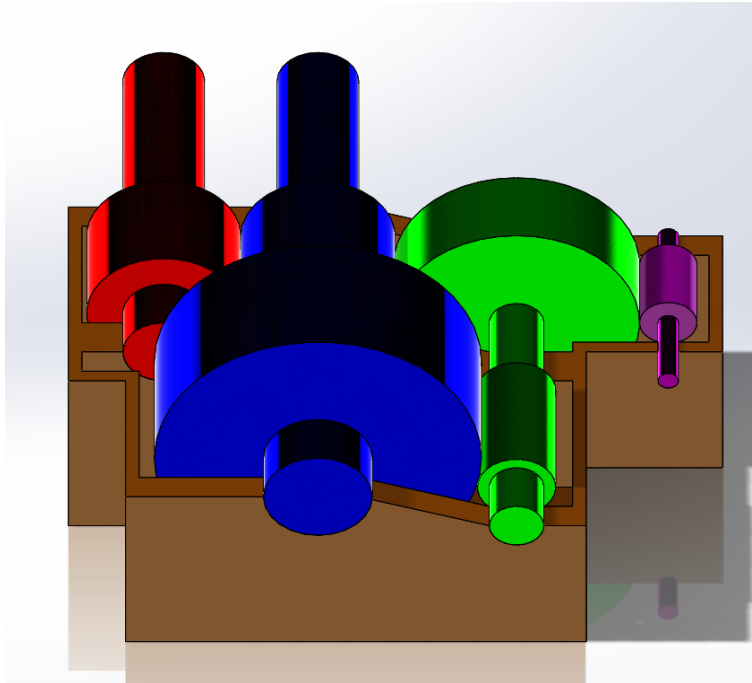


Figure 15: Rear view of the selected geartrain layout showing the compact design at the rear of the structure

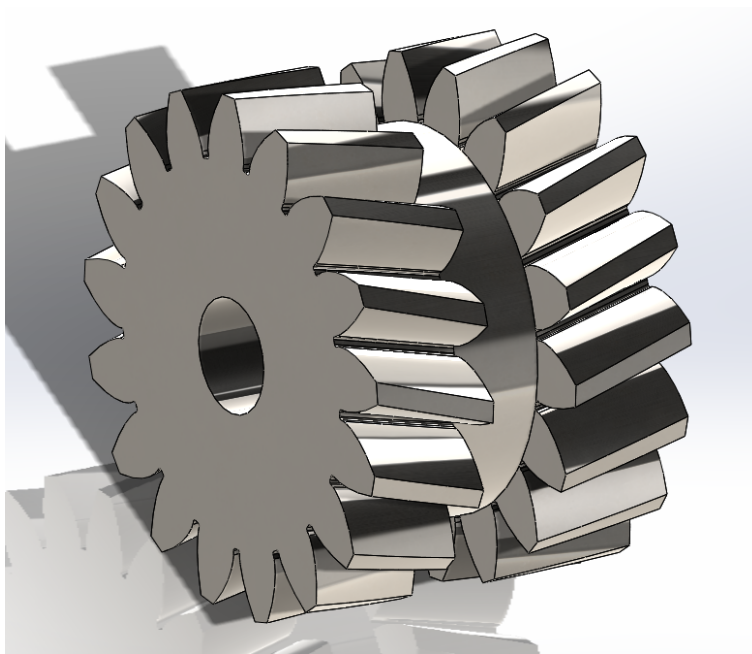


Figure 16: Screenshot of the detailed gear template, ready for MATLAB data to be imported

it may not show all of the features of the life size model, it will dramatically reduce the production time and require only glue for assembly. It will also be much more realistic to the assembly of the real product, assuming that is mainly constructed of sheet metal.

Shafts

Given the limited machining experience that our group members have and the fact that we have a few lathes and tools available to us, it has been decided that the shafts will be turned on a lathe. This allows for a higher precision and strength than could be achieved from 3D printing and gives a good starting point to base our model on. The advantages of the higher precision mean that excessive runout on the model is less likely to be an issue, and that the shafts should (in theory) fit nicely in the bearings.

Gears

The gears themselves will be 3D printed, to allow for the intricate shapes of helical gears to be produced. The cheap cost and relatively high strength of the components is also a plus. It does come with some limitations however; several tests have been devised to begin this week in order to establish the accuracy of the printers and what tolerances should be made to the 3D printed model to allow all of the parts to interact and mesh as planned. This is a process that may take a number of iterations, and with the availability of the printers expected to be limited in the coming weeks it has been decided to proceed with this step as soon as possible.

Keys, Seals, Bearings etc.

Should any keys be required for the shafts, they will most likely be 3D printed due to their small and precisely shaped nature. Specific seals will not be used on the prototype, however it is expected that sealed bearings will be used on all output/input shafts. In any case, attention to detail will be used to try and replicate any geometry on the prototype that clearly shows the fitment of a seal in the housing. The bearings are only available in selected sizes, so where possible the correct size will be used. Tradeoffs may have to be made however, and this should be taken into account before machining any shafts that they are expected to fit on.

7 Vibrational Analysis

7.1 Prospective Analysis

Lateral Analysis

A vibrational analysis will be performed upon the completion of the system. Utilizing both lateral and torsional analysis tools to determine the natural frequencies of the system. The lateral analysis will be performed by approximating each shaft as a simple beam and developing a mass spring model in accordance.

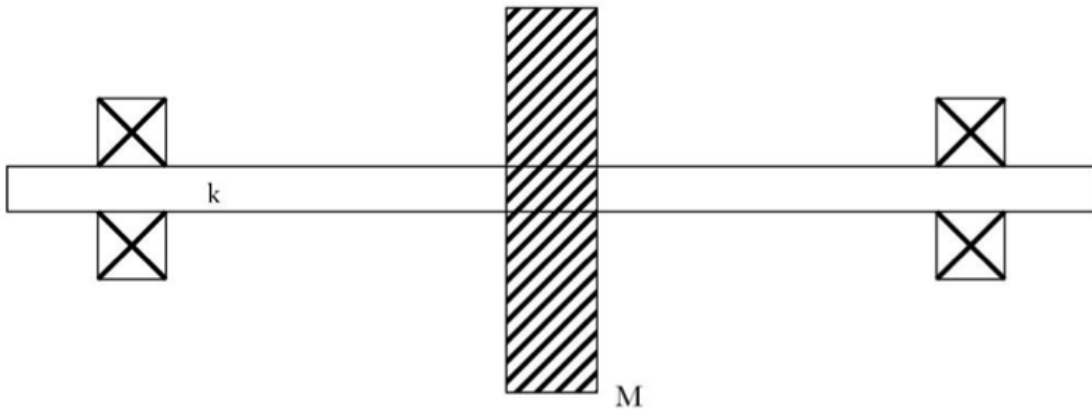


Figure 17: modal of mass spring system

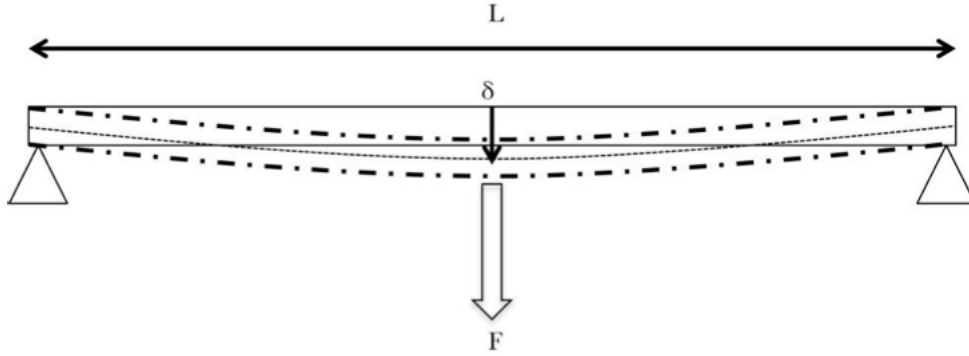


Figure 18: deflection of simple beam

The equation of motion $M\ddot{x} - c\dot{x} - Fx = 0$ will then be solved, ignoring the damping term, This leads to a natural frequency term being developed, resulting in

$$f_n = \frac{1}{2\pi} \sqrt{\frac{k}{M}} Hz$$

where k represented a spring constant, or the ratio between the force on the shaft and the maximum lateral deflection.

Torsional Analysis

In a similar manner, the natural frequency for rotation will be investigated. In this case, the system is approximated as a single mass on a cantilever beam. A different equation of motion will be implemented, $J_p\ddot{\theta} - C_T\dot{\theta} - k_T\theta = 0$ and again ignoring the damping term and solving produces the formula for natural frequency for rotation,

$$f_n' = \frac{1}{2\pi} \sqrt{\frac{k_t}{J_p}} Hz$$

where k_T is the rotational spring constant, the ratio between torque and maximum angular deflection. J_p represents the rotor polar moment of inertia.

We anticipate that when the rotation speeds for each shaft is compared to the corresponding natural frequency, either rotational or lateral, none of the rotation frequencies are a multiples of the natural frequency, which means that there will be no resonance of the shafts and so the system will be stable.

8 Thermal Analysis

To determine the operating temperature of the gearbox a power balance must be performed between the heat generated through friction within the gear box and the heat radiated away from the gearbox from the housing. It would also be possible if needed to use an active method of removing heat such as an additional radiator or oil pump, but for the developed gearbox this would not be necessary.

The process for determining the heats generated and lost is outlined in the AGMA standard 14179-1 Gear Reducers - Thermal Capacity. The heat generation is calculated as the sum of all individual gear mesh losses and all individual bearing losses, which are dependent upon the loads experienced by the gear teeth. There are also losses through factors such as the oil seals and churning losses. This is compared to the heat loss through the housing, which is a function of the thermal conductivity of the housing material and the outside temperature.

To calculate the heat lost through each gear pair, the relative sliding velocity must be calculated and then

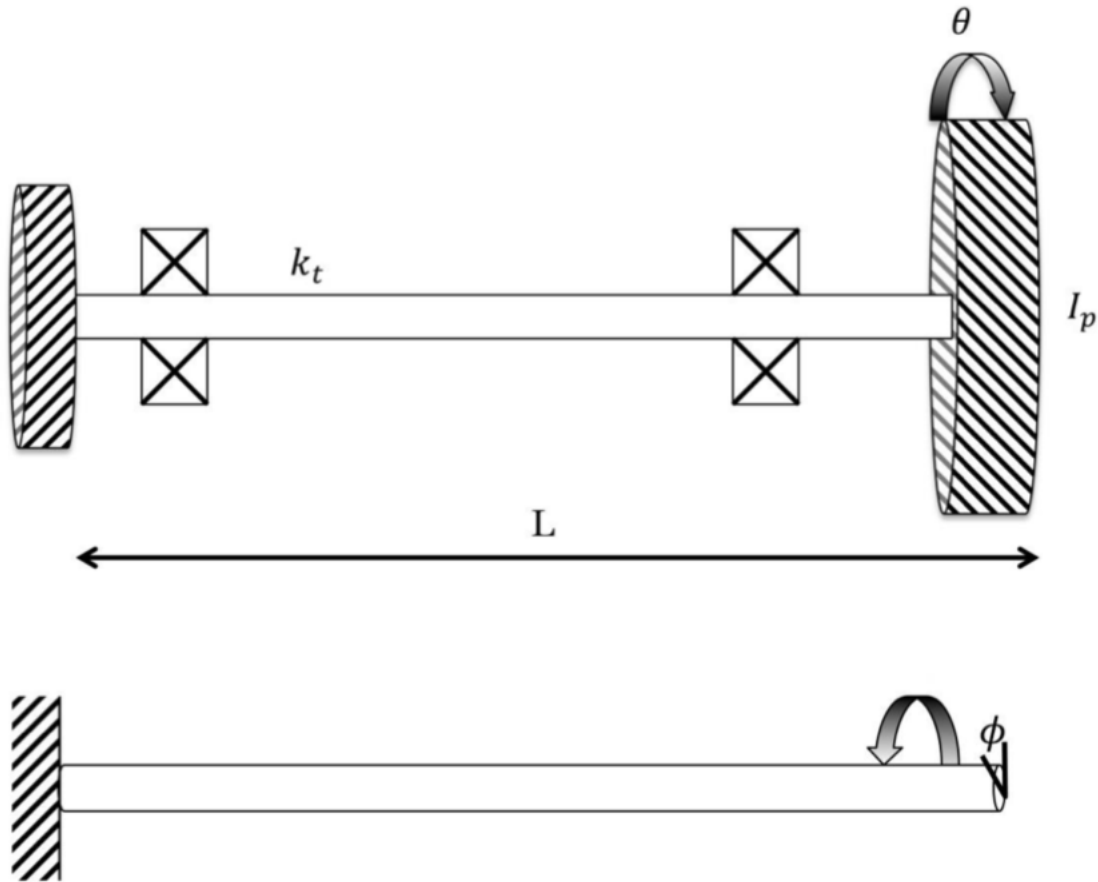


Figure 19: rotational vibration

multiplied by the sliding frictional force to achieve the power loss. The frictional force present is reliant upon the normal load upon the gear faces and the coefficient of friction. This then depends upon the lubrication properties and the material properties of the gears. As the gear teeth first approach each other and make contact they are initially sliding toward each other, however this will change as they part, reversing their velocity. This is compensated for in the calculations contained within the standard.

The heat transfer from the casing is dependent upon a number of variables, ranging from the ambient air temperature to the heat transfer rate between the oil and the casing, along with the air velocity across the outside surface. This is important to consider when deciding upon proper lubrication as the exterior conditions of the gearbox can vary greatly. There will likely be fluctuations in the outside air velocity, as well as large differences in the ambient temperature.

After careful considerations of the factors listed above, the designer will be able to develop a temperature balance to determine the operating temperature for the gearbox under standard conditions.

9 Progress Review

SIN Chart Discussion

Following the creation of a preliminary SIN chart it was deemed necessary that various additions and amendments were made. This is largely attributed to the teams' general gaps in knowledge in the early stages design, including selecting various tasks required for the successful design of a gearbox. The secondary SIN diagram outlines in further detail tasks such as preliminary gear design, selection of ratios, number of teeth, modules and henceforth diameters of gears. It then goes on to force analysis, which leads into material selection phases ensuring that the material of choice is both economically and technically feasible given the various constraints bestowed on us by the client. Further to that, the SIN diagram outlines the tasks involved in bearing selection with reference to catalog ratings and shaft sizes. It becomes very clear after a brief examination of the diagram that there is indeed an element of iteration necessary within the design phase of the project.

In conclusion, once the various gear, shaft, material and bearing information is obtained, the final stages involve a thermal and vibrational analysis of the gearbox. If the vibrational analysis is a success and the schematics match the preliminary design calculations, including the predetermined safety factor, then the gearbox is ready for manufacture. It was crucial for the team to be in possession of a detailed SIN chart as it greatly increases productivity, proper delegation of labor and ensures maximum efficiency within the group. When such a tool is used in combination with a Gantt chart, these various tasks can be kept track on not only on a basis of completion but on a scale of time as well. When certain goals and deadlines are not made, it calls for a team meeting where the mishaps can easily be pointed out and discussed.

Major Remaining Tasks

- Shaft Deflection calculations and research
- Detailed vibrational analysis calculations
- Optimization of gear sizes/geometry
- Further investigation into material and material treatment (i.e. hardening) selection for gears
- Further investigation into standards to ensure appropriate guidelines are followed
- Extensive procedure for gearbox assembly

Gantt Chart and hours

Throughout the project so far there has been much more time commitment required than first anticipated. This is evident from the difference between figure 21 and the figure 22 where the hourly breakdown of task completed is significantly higher. This required us to take make a change to our commitment.

In terms of how the team is tracking with regards to the initial Gantt chart, there is not a lot of time discrepancy. Shown in the appendices is both the original Gantt chart (46) and the revised chart (47). Extra time has been added for the initial layout and the geartrain and shaft preliminary design.

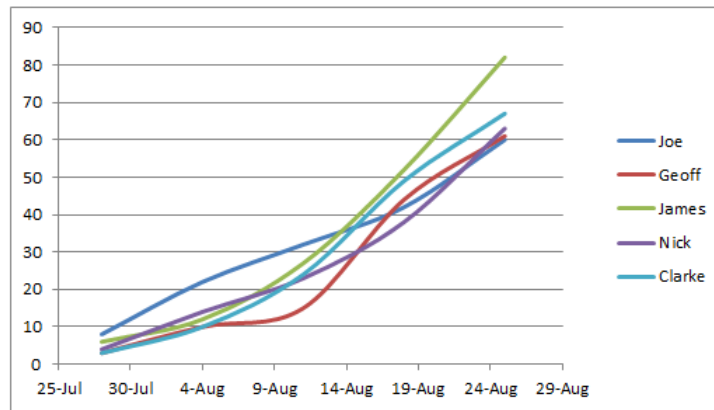


Figure 20: Graphical representation of each group members weekly hours

Hours											
Week Starting	Joe		Geoff		James		Nick		Clarke		Total
28-Jul	8	8	3	3	6	6	4	4	3	3	45
4-Aug	14	22	7	10	6	12	10	14	7	10	102
11-Aug	10	32	5	15	15	27	9	23	14	24	150
18-Aug	10	42	29	44	25	52	15	38	25	49	280
25-Aug	18	60	17	61	30	82	25	63	18	67	374
Total	60		61		82		63		67		951

Figure 21: Numerical breakdown of hours

Task:	Start Date	# Days	# Hrs Work	End Date
Realise Team Objectives & Constraints	28-Jul	14	70	11-Aug
Group Formation & Registration	28-Jul	3	15	31-Jul
Collect All Information Required (Objectives, Constraints etc)	31-Jul	5	25	5-Aug
Initial Appreciation & Layout	31-Jul	11	55	11-Aug
Initial Layout and Reduction Ratios Determined	1-Aug	10	50	11-Aug
Initial Appreciation & Layout Reporting Session	11-Aug	1	-	12-Aug
Conceptual Design Phase	12-Aug	31	155	12-Sep
Geartrain & Shaft Preliminary Design	12-Aug	12	60	24-Aug
Progress Report	12-Aug	20	100	1-Sep
Conduct Heat & Vibrational Analysis	24-Aug	12	60	5-Sep
Progress Report Session	1-Sep	1	-	2-Sep
Final Report	2-Sep	20	100	22-Sep
Design of Housing & Specification of Bearing & Seals	5-Sep	7	35	12-Sep
Production Phase	19-Sep	17	85	6-Oct
3D Modelling & Drawing	19-Sep	4	20	23-Sep
Completion Report	22-Sep	21	105	13-Oct
Component Production & Assembly	23-Sep	13	65	6-Oct
Completion Report Session	13-Oct	1	-	14-Oct

Figure 22: Task breakdown from IA

Task:	Start Date	# Days	# Hrs Work	End Date
Completion Report Session	13-Oct	1	-	14-Oct
Component Production & Assembly	23-Sep	13	65	6-Oct
Completion Report	22-Sep	21	105	13-Oct
3D Modelling & Drawing	19-Sep	4	20	23-Sep
Production Phase	19-Sep	17	85	6-Oct
Design of Housing & Specification of Bearing & Seals	5-Sep	7	35	12-Sep
Final Report	2-Sep	20	100	22-Sep
Progress Report Session	1-Sep	1	-	2-Sep
Conduct Heat & Vibrational Analysis	24-Aug	12	30	5-Sep
Progress Report	12-Aug	20	100	1-Sep
Geartrain & Shaft Preliminary Design	12-Aug	17	175	29-Aug
Initial Layout and Reduction Ratios Determined	12-Aug	11	55	23-Aug
Conceptual Design Phase	12-Aug	31	440	12-Sep
Initial Appreciation & Layout Reporting Session	11-Aug	1	-	12-Aug
Initial Appreciation & Layout	31-Jul	11	55	11-Aug
Collect All Information Required (Objectives, Constraints etc)	31-Jul	5	19	5-Aug
Group Formation & Registration	28-Jul	3	7	31-Jul
Realise Team Objectives & Constraints	28-Jul	14	81	11-Aug

Figure 23: Amended task breakdown

Appendices

A Minimum Volume Gear Design

By iterating the process and the formula from excerpt shown in figure: 24 it was possible to formulate the final gear ratio.

Major variables:

b=number of power paths (one for our selected design);

C_{m1} =load distribution factor for pitting resistance of the high speed mesh

C_{m2} =load distribution factor for pitting resistance of the low speed mesh

I_1 =geometry factor for pitting resistance of the high speed mesh

I_2 =geometry factor for pitting resistance of the low speed mesh

M_o =the overall gear ratio

M_{G1} =the high speed mesh gear ratio

$$X = m_{G1} \quad \dots(16)$$

$$A = \left(\frac{C_{m1}}{C_{m2}} \right) \left(\frac{I_2}{I_1} \right) \left(\frac{s_{ac2}}{s_{ac1}} \right)^2 \quad \dots(17)$$

$$B = 0.112 b^{0.126} \quad \dots(18)$$

$$C = 2.112 b^{0.112} \quad \dots(19)$$

And iterating this equation:

$$X1 = M_o \left\{ A \left[\left(\frac{B}{X^{0.888}} \right) + C X^{1.112} \right] + b \right\}^{-0.5} \quad \dots(20)$$

Figure 24: Formula for ratio calculation. Source: AGMA 901-A92

```

1  %pg references are to AGMA 901-A92
2  function min_vol_gearset()
3
4  %Function to iteratively solve the gear ratio for the high speed mesh and
5  %write it to the correct element of m_g.
6  %Using equations 16-20 (pg9) AGMA 901-A92
7
8  global m_G C_m I s_ac b M_o phi_n
9  setparameters %initialises parameters
10
11 for l=1:length(phi_n)
12 X = M_o^0.5; %initial approximation for X
13 m_G(1) = X; %initialise m_G
14 m_G(2) = M_o / m_G(1); %low speed mesh ratio initial approximation
15 error=1; %sets a variable to initialise the while loop
16
17 while error> 0.001 %iterates gear ratio until it converges to ideal ratio
18 for m=1:2 %calculates the geometry factors for 1 & 2 (ESTIMATE)
19 I(m) = (1+0.00682*(phi_n(l)*10) / 4.0584) * (m_G(m) / (m_G(m) + 1));
20 end
21
22 load_dist_factor %calculates load distribution factor for each mesh
23 A = (C_m(1)/C_m(2)) * (I(2)/I(1)) * (s_ac(2)/s_ac(1))^2;
24 B = 0.112 * (b^0.126);
25 C = 2.112 * (b^0.112);
26 X1 = M_o * (A * (B / (X^0.888)) + C * (X^1.112)) + b)^(-0.5);
27 error = abs(X-X1);
28 X = X1;
29 m_G(1) = X; %substitutes m_G(1) back in so variable can be written to txt
30 m_G(2) = M_o / m_G(1); %low speed mesh ratio updated
31 printTEST;
32 end
33 %shafttorques %calculates shaft torques so they are printed for each ratio
34 print_variables
35 end

```

Figure 25: Matlab code for ratio calculation part 1

Major assumptions made to produce the final ratio:

- Both meshes have the same allowable contact stress (same materials and treatment)
- Balanced pinion pitting ratings
- $C_v, C_H, C_a, C_s, C_s, C_f, C_p, C_T, C_R$ are constant for both meshes*

*Please see AGMA 901-A92 for variable descriptions.

```

36 - open gears.txt
37 - end
38
39 function load_dist_factor()
40 global m_G m_a C_a C_m T T_p n_i P_input b
41 %Function to iteratively calculate Load Distribution factor C_m and writes
42 %it to correct element of matrix.
43 %Dependent on mesh# (i), aspect ratio (m_a), application factor (C_a),
44 %transmitted pinion torque (T).
45 %From equation 9 (pg7) AGMA 901-A92
46
47 T(1) = P_input * 9550 / n_i; %initial estimates of torque since face width is not known first pinion (Nm)
48 T(2) = n_i / m_G(1); %torque estimate second pinion (Nm)
49
50 for j=1:1:2
51 %i=1 for high speed mesh
52 %i=2 for low speed mesh
53 T_p(j) = T(j)/b; %transmitted pinion torque
54 %Formulae for calculating aspect ratio
55 %from equation 4 (pg6) AGMA 901-A92)
56 m_a(j) = 2 * m_G(j) / (m_G(j) + 1); %aspect ratio (/2 for single helical or spur)
57 C_m(j) = 1 + m_a(j) * (0.2 + 0.0054 * (T_p(j) * C_a(j) / m_a(j))^0.33);
58 end
59 end

```

Figure 26: Matlab code for ratio calculation part 2

B Shafts

B.1 Australian Standard Shaft Equations

TABLE 2
FORMULAS FOR CALCULATING MINIMUM DIAMETER OF SHAFT D

Number of mechanism starts per year	Number of revolutions of shaft per year	Torque application conditions	Formula	Formulas
≤600	≤900	Manually or power applied	$D^3 = \frac{10^4 F_S}{F_Y} \sqrt{\left(M_q + \frac{P_q D}{8000}\right)^2 + \frac{3}{4} T_q^2}$	1
	>900	Power applied	$D^3 = \frac{10^4 F_S}{F_R} \sqrt{\left[K_S K \left(M_q + \frac{P_q D}{8000}\right)\right]^2 + \frac{3}{4} T_q^2}$	2
>600	>900	Power applied torque reversals	$D^3 = \frac{10^4 F_S}{F_R} K_S K \sqrt{\left(M_q + \frac{P_q D}{8000}\right)^2 + \frac{3}{4} T_q^2}$	3
		Power applied, no torque reversals (see Note 1)	$D^3 = \frac{10^4 F_S}{F_R} \sqrt{\left[K_S K \left(M_q + \frac{P_q D}{8000}\right)\right]^2 + \frac{3}{16} [(1 + K_S K) T_q]^2}$	4

NOTES:

- Where the magnitude of the torque in one direction is not greater than 0.1 times the torque in the other direction, the torque application conditions may be considered as being non-reversing.
- These formulas are extracted from a paper titled 'Shortcuts for Designing Shafts' by H.A. Borchardt, published in *Machine Design*, Vol. 45, No.3, 8 February 1973, pp 139-141.
- The value of F_R is based on 10^6 stress cycles and is applicable for numbers of revolutions of shafts per year greater than 50 000.
- For numbers of revolutions of shafts per year from 50 000 down to 900, formulas 2, 3 and 4 result in progressively more conservative values for the theoretical diameter of shaft.
- The value of F_S is 2.0 for Formula 1 and 1.2 for Formulas 2, 3 and 4. Where severe injury, death or extensive equipment damage is likely to occur because of the failure of the shaft, higher factors of safety may be used.
- The values of K_S , K and the term $P_q D/8000$ may require the calculation of a 'trial' diameter (see Appendix A).

Figure 27: Australian Standard AS 1403 Shaft Equations

B.2 Shaft Forces

Table 12: Shaft Forces (kN)

Shaft A	Gear 1	$F_{x\ 2,1}$	-24.78
		$F_{y\ 2,1}$	68.09
		$F_{z\ 2,1}$	0
Shaft B	Gear 2	$F_{x\ 1,2}$	24.78
		$F_{y\ 1,2}$	-68.09
		$F_{z\ 1,2}$	0
	Gear 3	$F_{x\ 4,3}$	-94.75
		$F_{y\ 4,3}$	-260.34
		$F_{z\ 4,3}$	0
Shaft C	Gear 4	$F_{x\ 3,4}$	94.75
		$F_{y\ 3,4}$	260.34
		$F_{z\ 3,4}$	0
	Gear 5	$F_{x\ 6,5}$	-233.00
		$F_{y\ 6,5}$	640.18
		$F_{z\ 6,5}$	0
Shaft D	Gear 6	$F_{x\ 5,6}$	233.00
		$F_{y\ 5,6}$	-640.18
		$F_{z\ 5,6}$	0

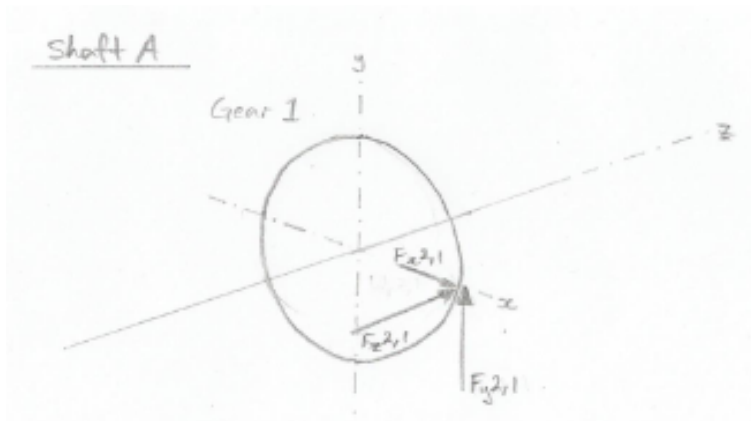


Figure 28: Shaft A

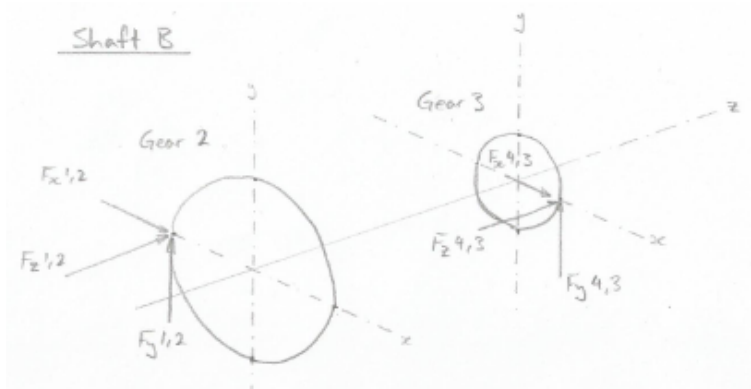


Figure 29: Shaft B

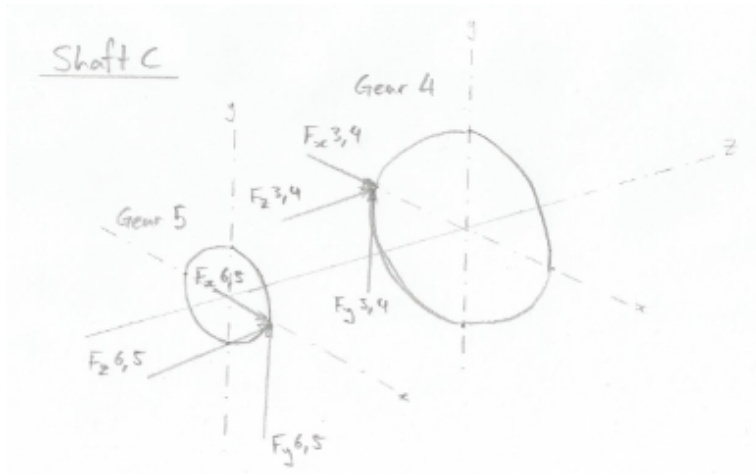


Figure 30: Shaft C

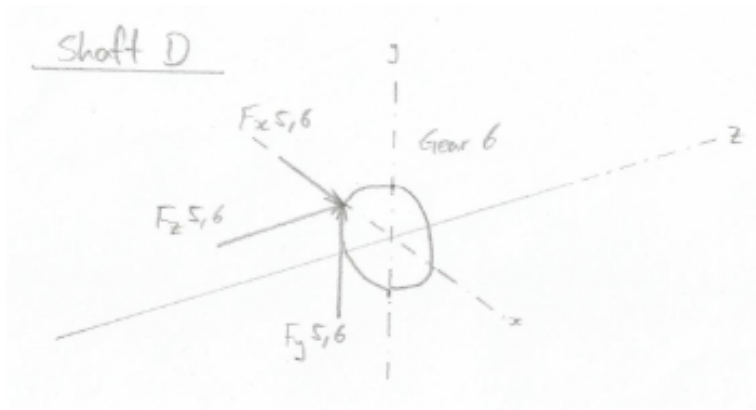


Figure 31: Shaft D

B.3 Shaft Free Body Diagrams

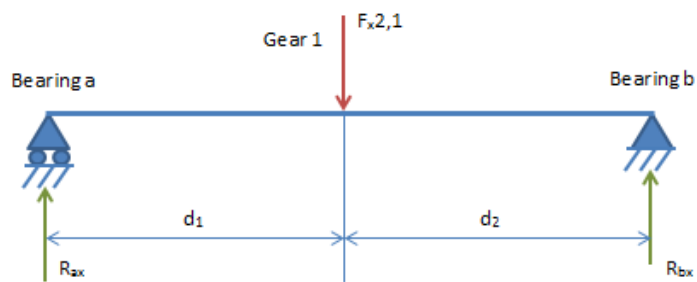


Figure 32: Shaft A x-z FBD

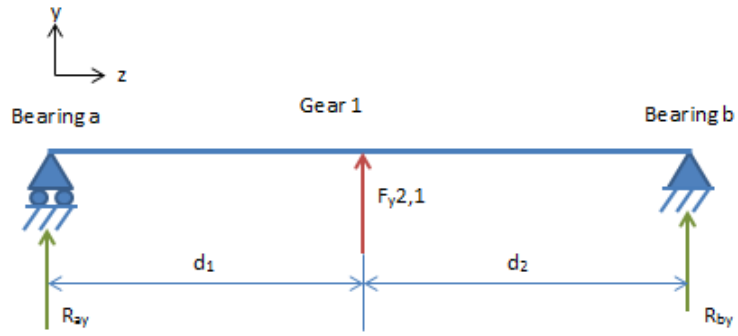


Figure 33: Shaft A y-z FBD

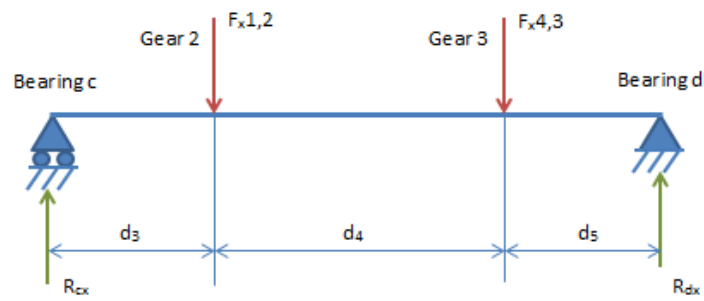


Figure 34: Shaft B x-z FBD

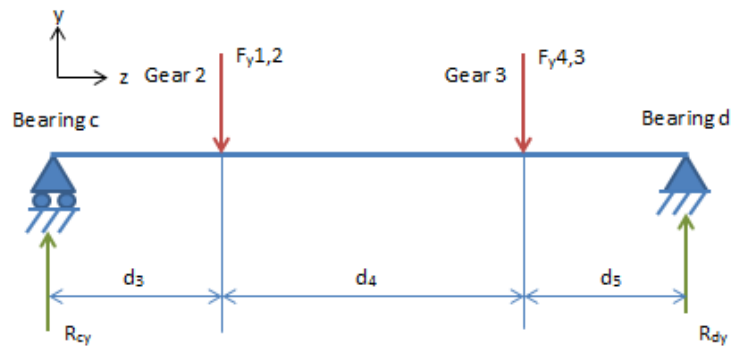


Figure 35: Shaft B y-z FBD

B.4 Shaft Bending Moment and Torque Diagrams

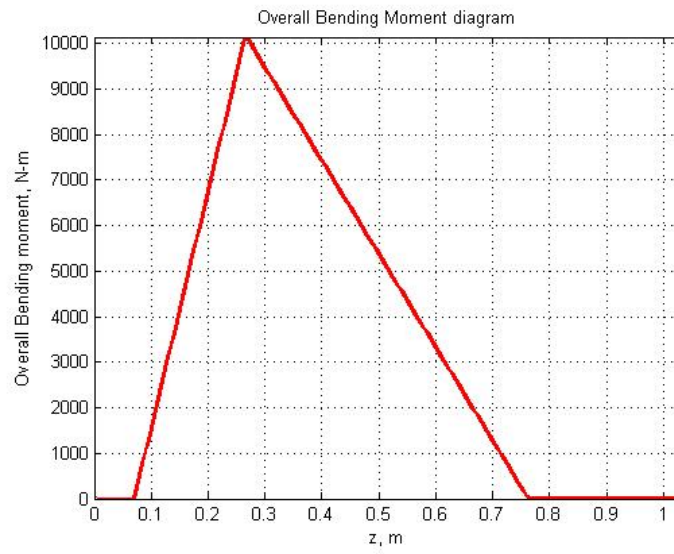


Figure 36: Shaft A Bending Moment Diagram

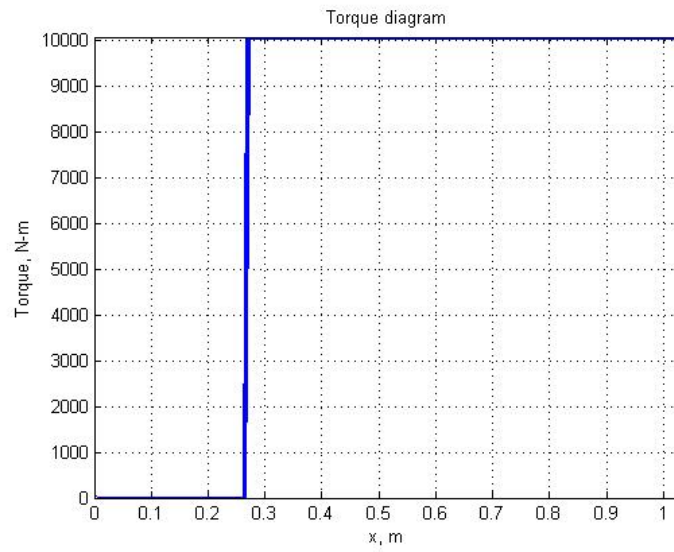


Figure 37: Shaft A Torque Diagram

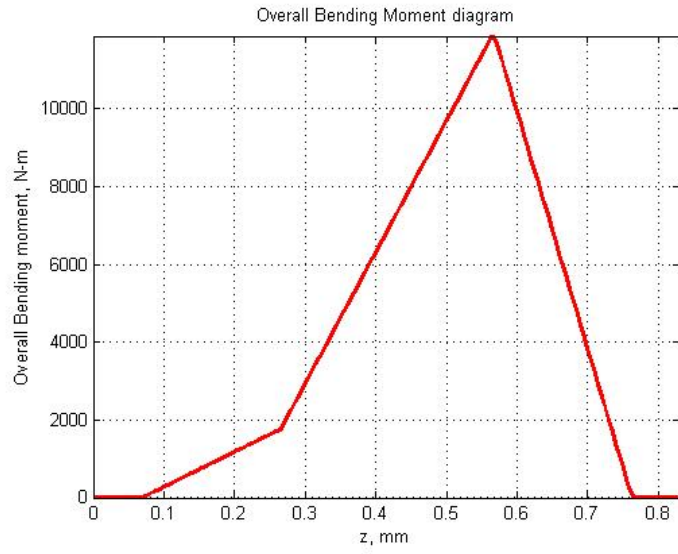


Figure 38: Shaft B Bending Moment Diagram

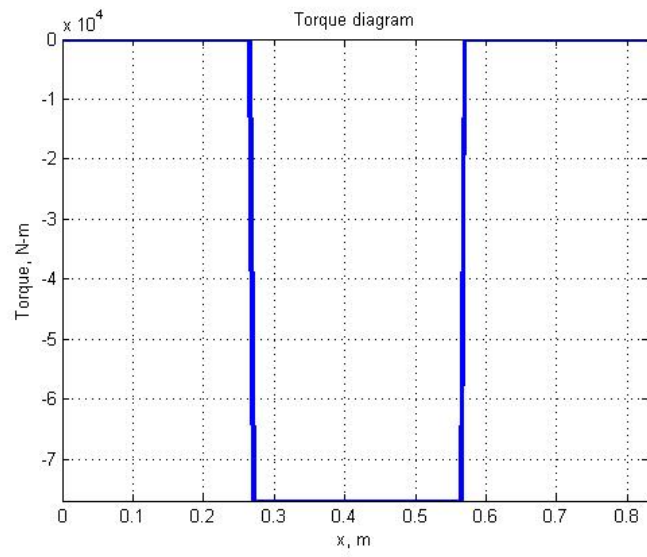


Figure 39: Shaft B Torque Diagram

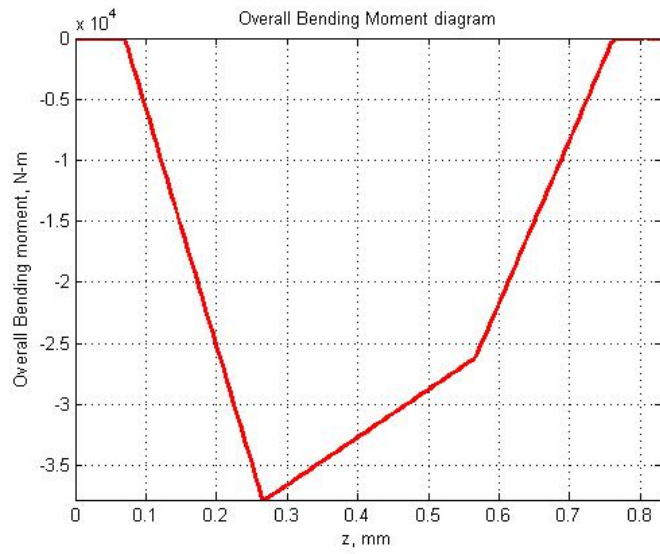


Figure 40: Shaft C Bending Moment Diagram

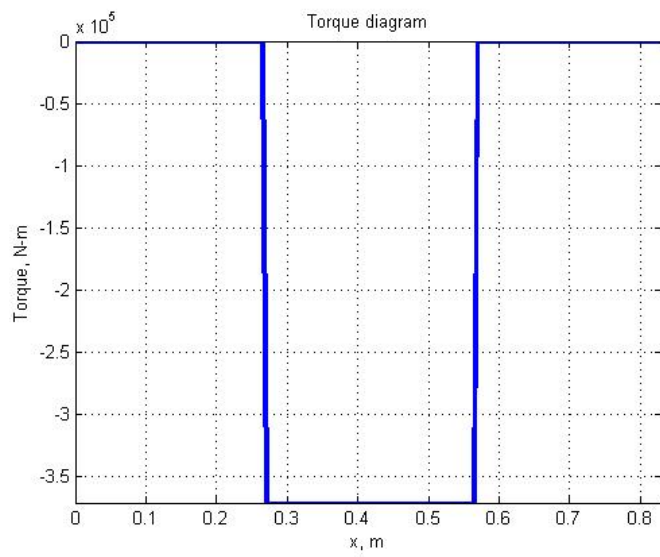


Figure 41: Shaft C Torque Diagram

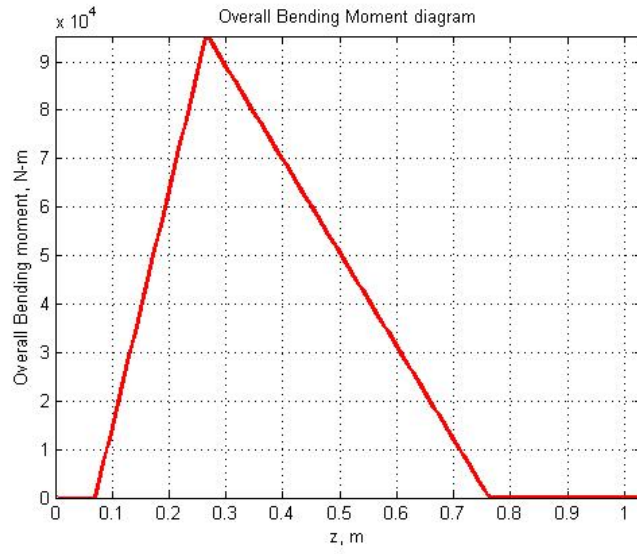


Figure 42: Shaft D Bending Moment Diagram

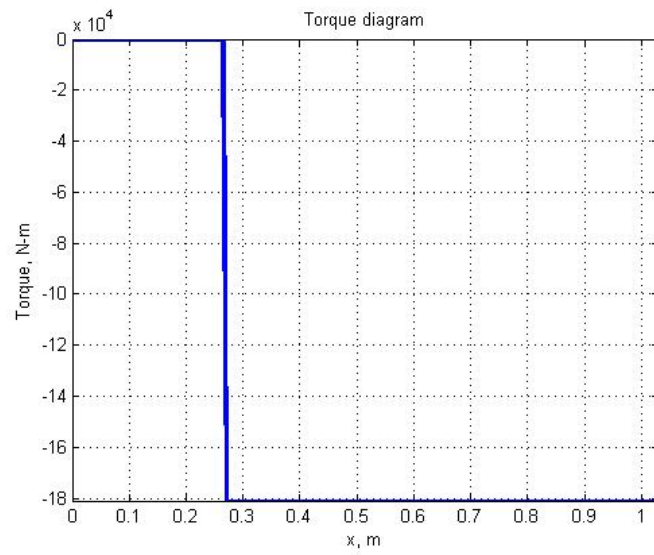


Figure 43: Shaft D Torque Diagram

C SIN Diagrams

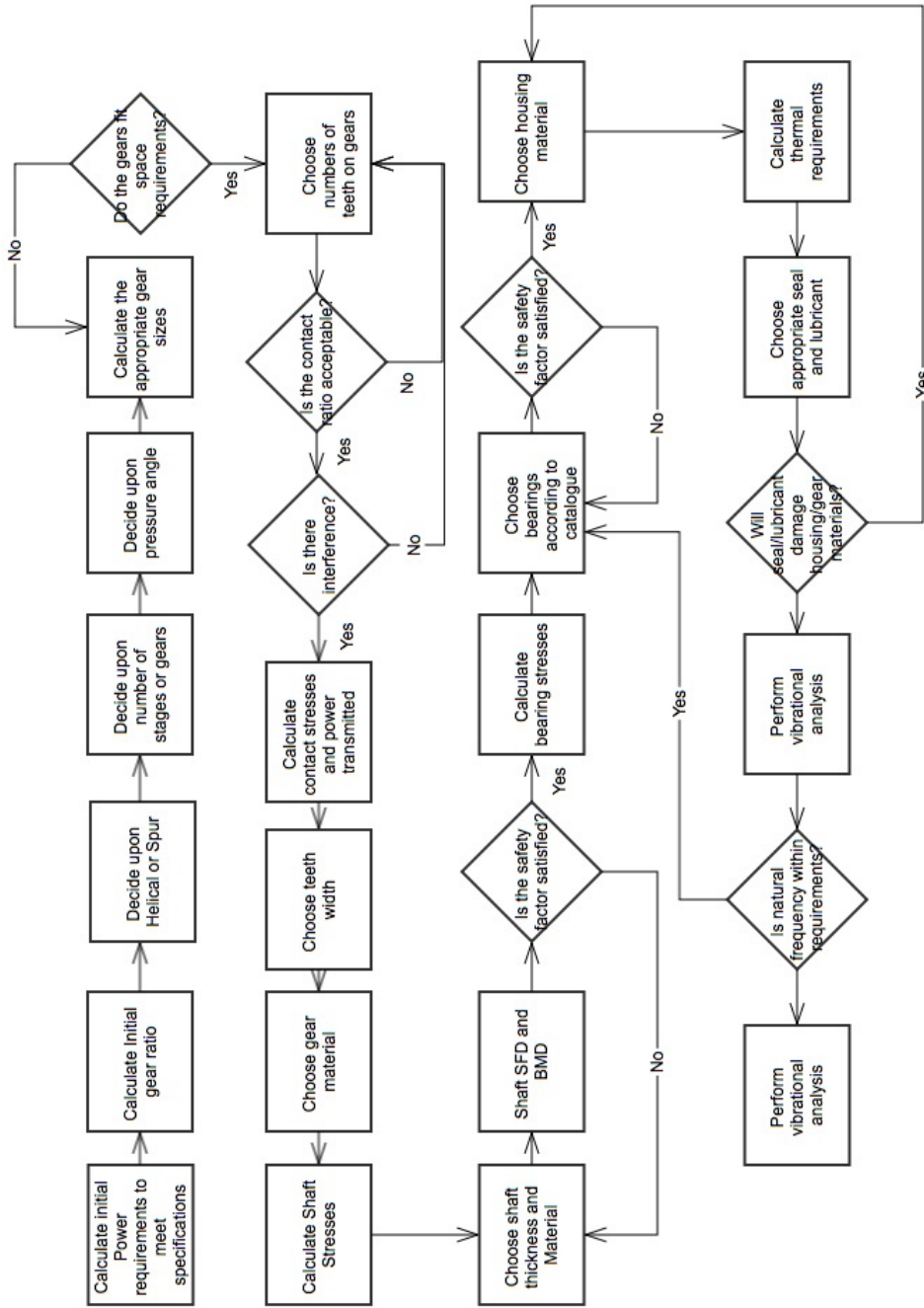


Figure 44: Preliminary SIN diagram

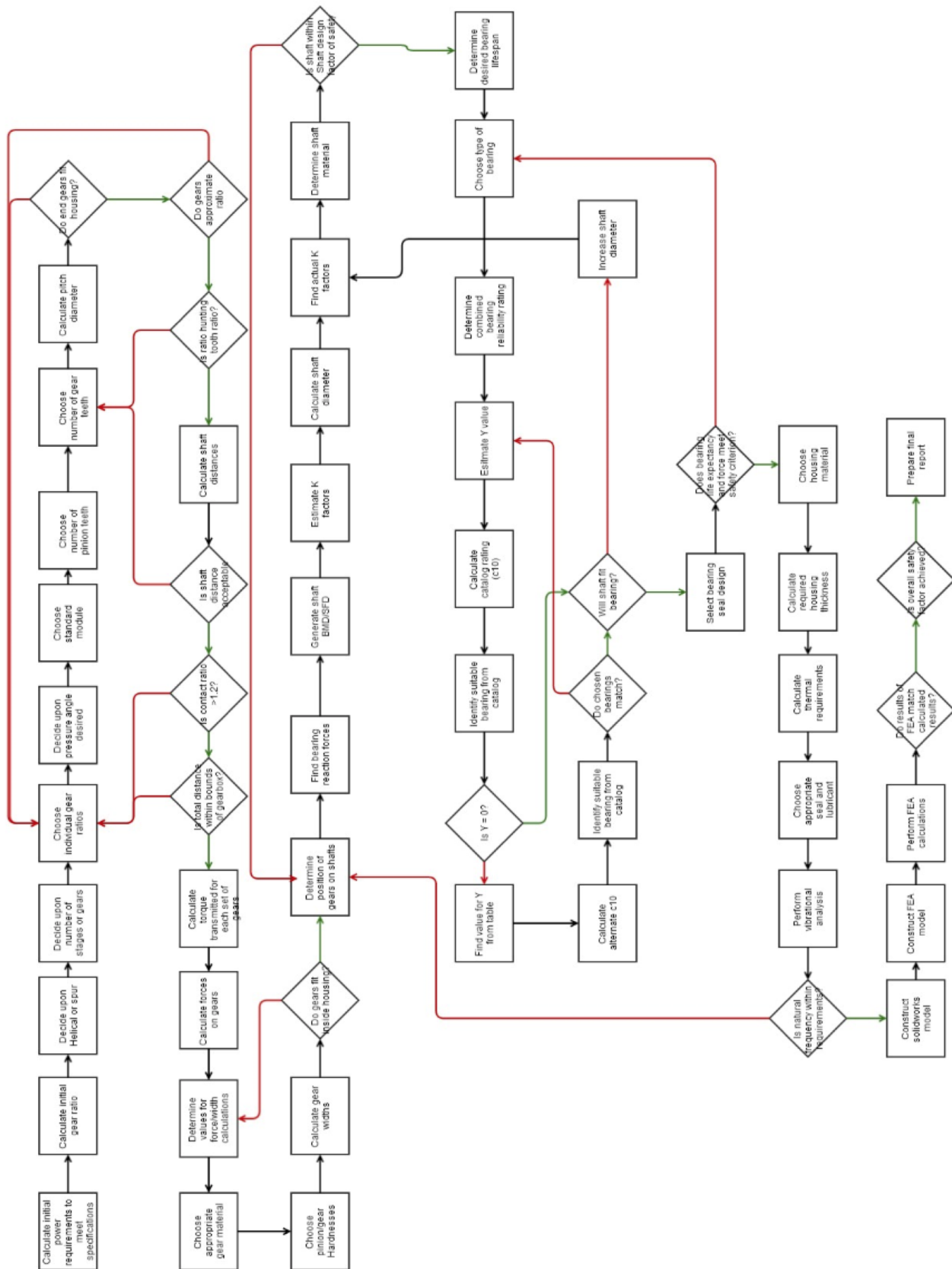


Figure 45: Secondary SIN diagram

D Gantt Charts

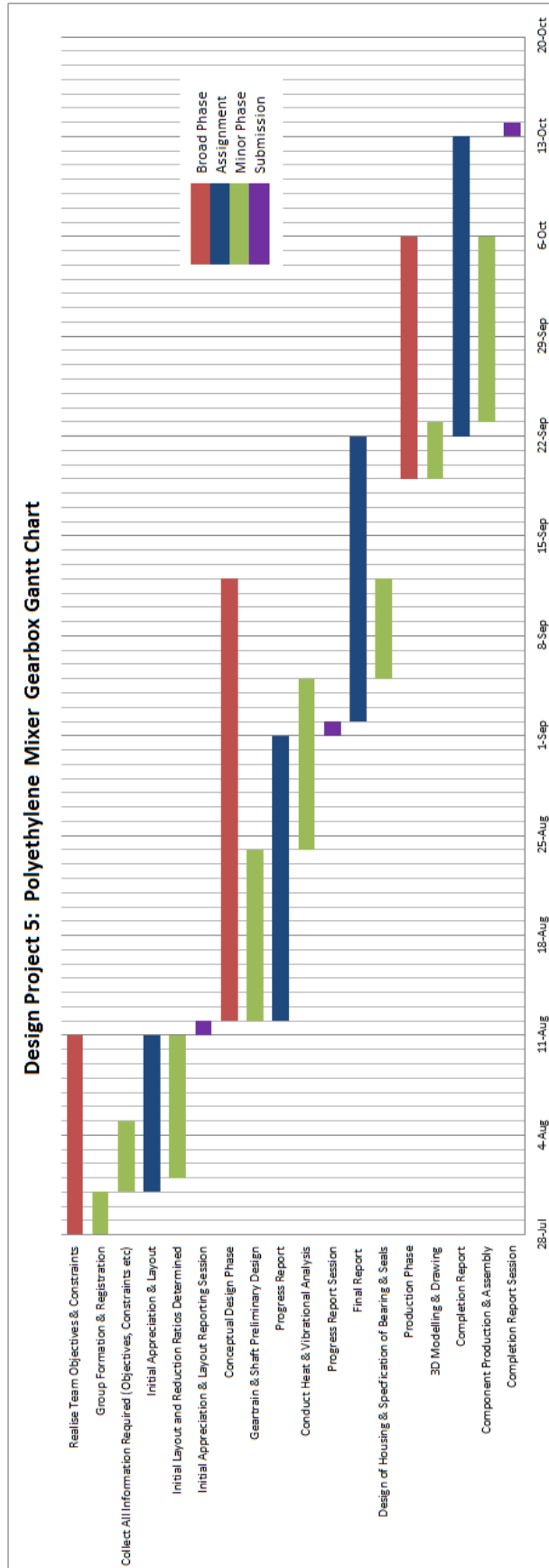


Figure 46: Gantt Chart as shown in the Initial Appreciation

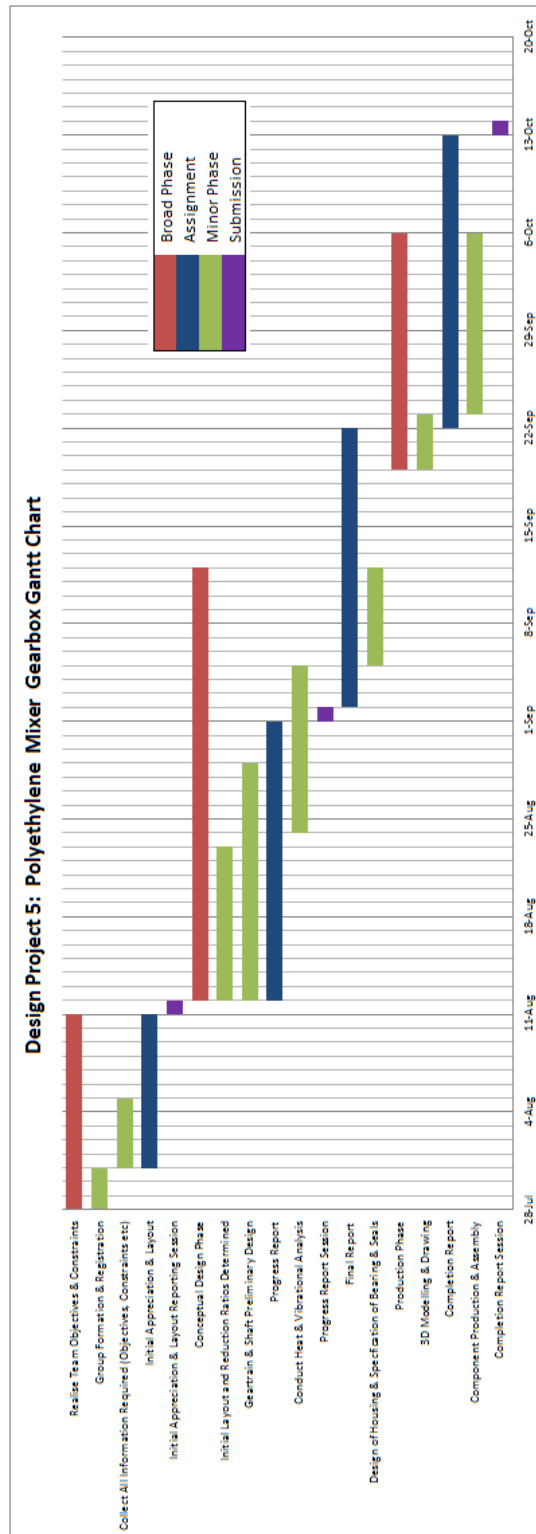


Figure 47: Revised Gantt Chart

E References

1. Budynas, R & Nisbett, J (2011), *Shigley's Mechanical Engineering Design: Ninth Edition in SI Units*, McGraw-Hill, New York.
2. *AGMA 908-B89: Geometry Factors for Determining the Pitting Resistance and Bending Strength of Spur, Helical and Herringbone Gear Teeth* (1999), American Gear Manufactures Association, Alexandria Virginia.
3. *AGMA 901-A92: A Rational Procedure for the Preliminary Design of Minimum Volume Gears* (1992), American Gear Manufactures Association, Alexandria Virginia.
4. *AS 1403-2004: Design of rotating steel shafts* (2004), Australian Standard